Iterated maps for annealed Boolean networks

Juha Kesseli,* Pauli Rämö, and Olli Yli-Harja
Institute of Signal Processing, Tampere University of Technology, P.O. Box 553, 33101 Tampere, Finland
(Received 15 March 2006; published 5 October 2006)

Boolean networks are used to study the large-scale properties of nonlinear systems and are mainly applied to model genetic regulatory networks. A statistical method called the annealed approximation is commonly used to examine the dynamical properties of randomly generated Boolean networks that are created with selected statistical features. However, in the literature there are several variations of the annealed approximation. These approximations cannot be interchangeably used in all cases due to different background assumptions. In this paper, we present the so-called four-state model, derive the different approximations from this model, and make the differences and connections between these approximations explicit. As an application of the presented results, we study the properties of the Boolean networks that are constructed with random functions, canalizing functions, and regulatory functions found in the biological literature.

DOI: 10.1103/PhysRevE.74.046104 PACS number(s): 89.75.Hc, 82.39.Rt, 05.45.−a, 87.16.Yc

I. INTRODUCTION

Kauffman originally introduced Boolean networks as simple models for large dimensional, nonlinear, and dynamical systems such as gene regulatory networks [1,2]. He observed that large randomly generated Boolean networks with suitable parameters can give rise to surprisingly ordered systems with a small set of states in which the system will end up. These final states constitute dynamical attractors that can be interpreted as cell types of an organism.

In addition to the attractors, we can study the dynamics of Boolean networks on a general level by examining the propagation of perturbations [3]. If small perturbations tend to die out, the networks are called ordered. If small perturbations have on average large effects on the system state, the networks are called chaotic. The intermediate case where perturbations retain on average their size is called critical. Recently, there has been evidence that real gene regulatory networks may have critical dynamics [4,5].

A significant breakthrough in the analysis of Boolean network dynamics has been the introduction of the so-called annealed approximation [6,7]. This statistical mean-field approximation allows the prediction of network dynamics for a given distribution of network update rules. The predictive information of the approximation can be given in the form of an iterative map that predicts the perturbation size at time $t+1$ given the perturbation size at time t. This approximation and other equivalent ones have been used for several different kinds of update functions [8,9].

However, the mapping as originally given does not perform well for all distributions of update functions. In particular, the original annealed approximation can classify as chaotic ordered networks that have many canalizing functions. Canalizing functions are interesting since they have been suggested as a candidate mechanism for order in networks with high connectivity [10]. In order to make the annealed approximation more accurate, we need to take into account the so-called forcing effect. Moreira *et al.* [11] studied networks with canalizing functions using a particular annealed approximation that takes the forcing effect into account. Kesseli *et al.* [12] proposed a slightly different version.

In this paper, we clearly show the connections and differences between the above-mentioned and the original annealed approximations by using a general model. We derive all three approximations as special cases of this model. In addition to being theoretically interesting, the model based on iterative maps could also be used as a more general approximation of Boolean network dynamics.

II. BASIC PROPERTIES OF BOOLEAN NETWORKS

A Boolean network is a directed graph with N nodes. Nodes represent, for example, genes, and graph arcs represent biochemical interactions between the genes. The in-degree of a node is the number of incoming connections to the node, and the out-degree is the number of outgoing connections. We denote the distribution of node in-degrees k as p_k and the expected in-degree as $\langle p_k \rangle$. Each node is assigned a binary-state variable and a Boolean function as an update rule. The inputs of each update rule are assigned according to the graph connections. The value 1 of the state represents an active gene, while the value 0 represents a nonactive gene. The Boolean function f associated with the node represents the biochemical rule of regulatory interactions affecting the gene in question. Boolean functions can be presented in truth table format. For example, $f=[00111000]$ refers to the function f with three input variables x_1, x_2, and x_3:

x_1	x_2	x_3	$f(x)$
0	0	0	0
0	0	1	0
0	1	0	1
0	1	1	1
1	0	0	1
1	0	1	0
1	1	0	0
1	1	1	0

*Electronic address: kesseli@cs.tut.fi

We denote the distribution over the set of functions in the network as $\mathfrak{F}$ and the distribution of functions with given in-degree k as $\mathfrak{F}_k$. The in-degree and function distributions are connected in such a way that the degree distribution of the function distribution matches the network in-degree distribution. The state of the network is the vector of the state variable values of all the nodes at a given time instant. The network nodes are updated synchronously.

In our analysis, we use the annealed approximation. This means that we let the network size N approach infinity and shuffle the network connections and functions after every time step. In addition, we assume that the network topology is random; i.e., the inputs to a node are chosen randomly among all other nodes. The approximations of annealed dynamics and random topology allow us to use simple probabilistic methods to analyze the dynamical behavior of the network. Of course, real gene regulatory networks cannot be expected to have a random topology. Further research is needed to understand the dynamical behavior of Boolean networks with more realistic topological properties. We refer to finite-size Boolean networks with fixed connections and functions as quenched Boolean networks.

In a deterministic system with a finite state space any trajectory will ultimately come back to a state visited earlier and start repeating a sequence of states called an attractor. In practice, one of the main differences between quenched and annealed networks is the absence of attractors in the latter. The properties of attractors have been widely studied in the literature [13,14].

Biological observations have suggested that the in-degree distribution of real gene regulatory networks may be close to the Poisson distribution [15]

$$p_k = \frac{K^k}{k!} e^{-K}.$$

Here, K is the distribution parameter. For a Poisson distribution $\langle p_k \rangle = K$. Other studies suggest that the in-degree distribution might be a power law [16] of the form

$$p_k = \frac{1}{\zeta(\gamma)} k^{-\gamma}, \quad p_0 = 1 - \frac{\zeta(\gamma)}{\zeta(\gamma - 1)}.$$

Here, γ is the distribution parameter and $\zeta(\gamma)$ is the Riemann zeta function. For a power-law distribution the average in-degree is

$$\langle p_k \rangle = \frac{\zeta(\gamma - 1)}{\zeta(\gamma)}.$$

Let us now consider the probability that a node has value 1 if we know this probability in the previous time step in the annealed network. We call this mapping $g(b)$ the bias map of the function distribution. The mapping is given by

$$g(b) = \underset{f \in \mathfrak{F}}{E} \left[\sum_{x \in \{0,1\}^{K_f}} f(x) P(x|b) \right],$$

where

$$P(x|b) = b^{|x|}(1-b)^{K_f - |x|}$$

is the probability for any fixed input vector $x \in \{0,1\}^{K_f}$, given that we know the probability b for an arbitrary element of the input vector to have value 1. Here, K_f is the in-degree of the function f that is drawn from a desired function distribution $\mathfrak{F}$ and $|x|$ is the number of 1's in the vector x. The bias map can be iterated by

$$b_{t+1} = g(b_t).$$

This mapping may have nontrivial fixed-point solutions depending on the chosen function distribution [17–20]. However, it can be assumed that all biologically realistic function distributions finally reach a unique stable fixed point $b^* = g(b^*)$ [17]. If this is not the case, many results in this paper do not apply directly. The derivative of the bias map is

$$g'(b) = \underset{f \in \mathfrak{F}}{E} \left[\sum_{x \in \{0,1\}^{K_f}} f(x) \frac{|x| - K_f b}{b(1-b)} P(x|b) \right].$$

The average influence of a function is the probability that the function changes its output if we flip the value of an input. In addition, we assume that an input has value 1 with probability b. For a function distribution the average influence $I(b)$ is

$$I(b) = \underset{f \in \mathfrak{F}}{E} \left[\frac{1}{K_f} \sum_{i=1}^{K_f} \sum_{x \in \{0,1\}^{K_f}} [f(x) \oplus f(x \oplus e_i)] P(x|b) \right].$$

Here, $\oplus$ refers to an XOR operator and e_i is the unit vector of length K_f with $|e_i| = 1$ and value 1 in the ith position. Note that the middle part of the equation can be expressed also with a Boolean derivative:

$$\frac{\delta f(x)}{\delta x_i} = f(x) \oplus f(x \oplus e_i).$$

We define the average influence I of the function distribution $\mathfrak{F}$ at the bias-map fixed point b^* as

$$I = I(b^*).$$

The average influence I can be considered as the average probability that an arbitrary arc is propagating a perturbation at the bias-map fixed-point state. The influence of the ith component of the input vector x is defined as

$$I_i(b) = \sum_{x \in \{0,1\}^{K_f}} [f(x) \oplus f(x \oplus e_i)] P(x|b).$$

The average sensitivity of a Boolean function is the sum of the influences $I_i(b)$. The average sensitivity of a function distribution is given by

$$\lambda(b) = \underset{f \in \mathfrak{F}}{E} \left[\sum_{i=1}^{K_f} \sum_{x \in \{0,1\}^{K_f}} [f(x) \oplus f(x \oplus e_i)] P(x|b) \right].$$

By using the average sensitivity at the bias-map fixed point we can define the network's order parameter as

$$\lambda = \lambda(b^*).$$

The order parameter λ is the average amount of nodes that are perturbed one time step after we have flipped the value of

a randomly chosen node, given that the network has reached the bias-map fixed point before the perturbation. Networks with $\lambda<1$ are stable, networks with $\lambda=1$ are critical, and networks with $\lambda>1$ are chaotic. The average sensitivity $\lambda(\frac{1}{2})$ has been previously used as a measure of dynamical behavior [9]. As will be confirmed by the Derrida maps derived in Sec. III, this measure is not generally suitable when studying, for example, canalizing functions.

In some applications we need to divide the parameter $\lambda(b)$ into two parts $\lambda_C(b)$ and $\lambda_I(b)$. These parts correspond to the average amount of nodes that copy or invert the value of the perturbed node:

$$\lambda_C(b) = \underset{f\in\mathfrak{F}}{E}\left[\sum_{i=1}^{K_f}\sum_{x\in\{0,1\}^{K_f}}\{(1-x_i)[1-f(x)]f(x\oplus e_i) + x_i f(x)[1-f(x\oplus e_i)]\}P(x|b)\right],$$

$$\lambda_I(b) = \underset{f\in\mathfrak{F}}{E}\left[\sum_{i=1}^{K_f}\sum_{x\in\{0,1\}^{K_f}}\{(1-x_i)f(x)[1-f(x\oplus e_i)] + x_i[1-f(x)]f(x\oplus e_i)\}P(x|b)\right].$$

It can be noted that

$$\lambda(b) = \lambda_C(b) + \lambda_I(b).$$

We define λ_C and λ_I at the bias-map fixed point as

$$\lambda_C = \lambda_C(b^*), \quad \lambda_I = \lambda_I(b^*).$$

We define $\Delta\lambda(b)$ as the difference between $\lambda_C(b)$ and $\lambda_I(b)$:

$$\Delta\lambda(b) = \lambda_C(b) - \lambda_I(b).$$

Note that $\Delta\lambda(b)$ is the derivative of the bias map at b:

$$\Delta\lambda(b) = g'(b).$$

The proof is given in the Appendix. It follows that $\Delta\lambda$ at the bias-map fixed point can be given simply as

$$\Delta\lambda = g'(b^*).$$

It has been found that the parameter $\Delta\lambda$ is important, for example, in determining the number of attractors and their lengths in quenched Boolean networks [13].

III. DERRIDA MAPS

Let us consider the situation where we have two annealed networks running in parallel; see Fig. 1. Network 1 represents the network without a perturbation. Instead, in network 2 a certain fraction of the nodes is perturbed (the node values are opposite to those of network 1). Both networks have the same functions and connections at each time step. Each pair of nodes may have four different combinations of values (00, 01, 10, and 11). For example, we can now define $p_{00}(t)$ as the probability that at time t a randomly selected node has value

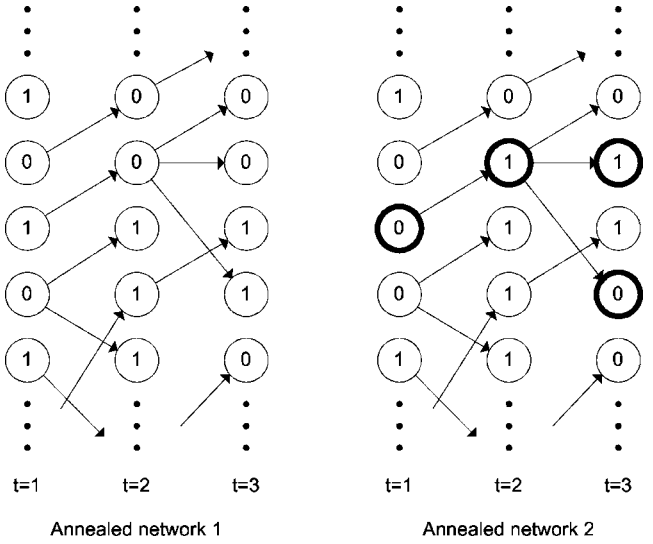

FIG. 1. An illustration of the model where two annealed networks run in parallel. Highlighted nodes represent nodes that are perturbed.

0 in both networks. Corresponding definitions can be given for all the combinations. The probabilities p_{00}, p_{01}, p_{10}, and p_{11} can be updated according to the following maps:

$$p_{00}(t+1) = \underset{f\in\mathfrak{F}}{E}\left[\sum_{x\in\{0,1\}^{K_f}}\sum_{y\in\{0,1\}^{K_f}}[1-f(x)][1-f(y)]P(x,y,t)\right],$$

$$p_{01}(t+1) = \underset{f\in\mathfrak{F}}{E}\left[\sum_{x\in\{0,1\}^{K_f}}\sum_{y\in\{0,1\}^{K_f}}[1-f(x)]f(y)P(x,y,t)\right],$$

$$p_{10}(t+1) = \underset{f\in\mathfrak{F}}{E}\left[\sum_{x\in\{0,1\}^{K_f}}\sum_{y\in\{0,1\}^{K_f}}f(x)[1-f(y)]P(x,y,t)\right],$$

$$p_{11}(t+1) = \underset{f\in\mathfrak{F}}{E}\left[\sum_{x\in\{0,1\}^{K_f}}\sum_{y\in\{0,1\}^{K_f}}f(x)f(y)P(x,y,t)\right],$$

where

$$P(x,y,t) = p_{00}(t)^{(1-x)^T(1-y)}p_{01}(t)^{(1-x)^T y}p_{10}(t)^{x^T(1-y)}p_{11}(t)^{x^T y}.$$

The sum of these probabilities naturally adds up to 1—i.e., $p_{00}+p_{01}+p_{10}+p_{11}=1$. For this reason, three of the above iterative mappings are needed to completely describe the annealed model. We call this model of network dynamics the four-state model. We define b_1 as the probability that a node has value 1 in annealed network 1 and b_2 as the probability that a node has value 1 in annealed network 2 at time t. ρ is the probability that a pair of nodes has different values. In other words, the proportion of perturbed nodes ρ is the perturbation size in the network. We find that the connections between these probabilities are

$$b_1 = p_{10} + p_{11},$$

$$b_2 = p_{01} + p_{11},$$

$$\rho = p_{10} + p_{01},$$

and conversely,

$$p_{00} = 1 - \frac{1}{2}(b_1 + b_2 + \rho),$$

$$p_{01} = \frac{1}{2}(b_2 - b_1 + \rho),$$

$$p_{10} = \frac{1}{2}(b_1 - b_2 + \rho),$$

$$p_{11} = \frac{1}{2}(b_1 + b_2 - \rho).$$

It is usually more illustrative to use b_1, b_2, and ρ instead of the probabilities p_{ij}. Derrida maps have been commonly used to depict the propagation of perturbations in the network [6]:

$$h(\rho) = \underset{f\in\mathfrak{F}}{E}\left[\sum_{x\in\{0,1\}^{K_f}}\sum_{y\in\{0,1\}^{K_f}}[f(x)\oplus f(y)]P(x,y,t)\right].$$

We are interested in the fixed point $\rho^*=h(\rho^*)$ of the Derrida map. If $\rho^*=0$, the network is stable because all perturbations eventually die out. If $\rho^*>0$, the network is chaotic because small enough differences in state will always be amplified according to the approximation. Since the Derrida maps are one dimensional, some information about the dynamical behavior of the four-state model that needs three iterative mappings must be omitted. In particular, we assume that the bias map has a unique stable fixed point for the given function distribution. In the most commonly used definition, the network biases b_1 and b_2 are chosen to be $1/2$, meaning that the perturbations are studied in states selected randomly with equal probability for all the possible states. Using this assumption we get $h_1(\rho)$ as

$$h_1(\rho) = \underset{f\in\mathfrak{F}}{E}\left[\sum_{x\in\{0,1\}^{K_f}}\sum_{y\in\{0,1\}^{K_f}}[f(x)\oplus f(y)]\left(\frac{1}{2}-\frac{1}{2}\rho\right)^{K_f-|x\oplus y|}\times\left(\frac{1}{2}\rho\right)^{|x\oplus y|}\right].$$

The Derrida map $h_1(\rho)$ does not give correct estimates for the fixed point ρ^*, because the effects caused by the change of network bias are not taken into account. As the second case, we choose the initial state so that a node has value 1 with probability b^* and let the perturbed state have the average perturbed bias—i.e., $b_1=b^*$ and $b_2=b^*-2b^*\rho+\rho$. Using this assumption we get $h_2(\rho)$ as

$$h_2(\rho) = \underset{f\in\mathfrak{F}}{E}\left[\sum_{x\in\{0,1\}^{K_f}}\sum_{y\in\{0,1\}^{K_f}}[f(x)\oplus f(y)]\times\cdots\times(1-b^*+b^*\rho-\rho)^{(1-x)^T(1-y)}(b^*-b^*\rho)^{x^Ty}(\rho-b^*\rho)^{(1-x)^Ty}(b^*\rho)^{x^T(1-y)}\right].$$

This expression can be simplified as

$$h_2(\rho) = \underset{f\in\mathfrak{F}}{E}\left[\sum_{k=1}^{K_f}\lambda_k\rho^k(1-\rho)^{K_f-k}\right], \quad (1)$$

where

$$\lambda_k = \sum_{x\in\{0,1\}^{K_f}}\sum_{y\in P_k}[f(x)\oplus f(x\oplus y)]P(x|b^*)$$

is the average sensitivity of the function f over k variables. λ_k is also called the generalized sensitivity in [21]. Here, P_k refers to the set of all vectors $y\in\{0,1\}^{K_f}$ with $|y|=k$. The proof for this result is in the Appendix. This definition for the Derrida map has been used, for example, by Moreira *et al.* [11]. The fixed point ρ^* of the map is not correct because the second annealed network will not stay at the initial bias value given by the definition. In the special case of $b^*=0$ we note that this Derrida map is the same as the bias map

$$h_2(\rho) = g(\rho). \quad (2)$$

The proof is given in the Appendix. As a third option, we assume that $b_1=b_2=b^*$. In other words, we only make such perturbations that lead to the same bias for the second annealed network. The Derrida map $h_3(\rho)$ is

$$h_3(\rho) = \underset{f\in\mathfrak{F}}{E}\left[\sum_{x\in\{0,1\}^{K_f}}\sum_{y\in\{0,1\}^{K_f}}[f(x)\oplus f(y)]\times\left(1-b^*-\frac{1}{2}\rho\right)^{(1-x)^T(1-y)}\left(b^*-\frac{1}{2}\rho\right)^{x^Ty}\left(\frac{1}{2}\rho\right)^{|x\oplus y|}\right].$$

This map was presented in [12] in an alternative form. The fixed point ρ^* is correctly given by the Derrida map $h_3(\rho)$ because at the fixed point ρ^* both annealed networks have also reached their bias-map fixed points $b_1=b_2=b^*$. However, by using this definition, the maximum perturbation size that can be drawn is $\min(2b^*, 2-2b^*)$. This clearly discourages the use of $h_3(\rho)$ as a general one-dimensional map for predicting perturbation propagation. However, $h_3(\rho)$ can be used for visualization purposes. The slope of the Derrida map at the origin is often used as an order parameter for Boolean networks. We find that

$$h_1'(0) = \lambda\left(\frac{1}{2}\right). \quad (3)$$

The slopes at the origin for h_2 and h_3 Derrida maps are

$$h_2'(0) = h_3'(0) = \lambda. \quad (4)$$

Proofs of these results are in the Appendix. As confirmed by these observations, Derrida maps cannot give a complete description of the propagation of large perturbations in annealed Boolean networks. However, Derrida maps can still be used for visualization or other specific purposes when the limitations are taken into account.

IV. APPLICATIONS FOR RANDOM AND CANALIZING FUNCTIONS

In the context of Boolean and gene regulatory networks, two types of function distributions are of particular interest.

These are distributions of random functions and distributions with canalizing functions. We define the distribution of random functions with the parameter p that is the probability that an arbitrary entry in the truth table of the function is 1. Different networks can also be obtained by changing the distribution of in-degrees p_k.

The bias map for random functions is constant:

$$g(b) = p. \tag{5}$$

It follows that the bias-map fixed point $b^* = p$ and $\Delta\lambda = 0$. It can be seen that

$$\lambda(b) = 2p(1-p)\langle p_k \rangle. \tag{6}$$

Therefore, the order parameter $\lambda = 2p(1-p)\langle p_k \rangle$. We find that the Derrida maps $h_1(\rho)$, $h_2(\rho)$, and $h_3(\rho)$ are all equal for random functions and are given by

$$h(\rho) = 2p(1-p)\sum_{k=1}^{\infty} p_k[1-(1-\rho)^k]. \tag{7}$$

Proofs of these results can be found in the Appendix. We note that the form of the Derrida map depends not only on the average in-degree but also on the in-degree distribution. However, the slope of the map at the origin depends only on the average in-degree. With a straightforward application of the above, we find that the Derrida map for networks with a Poisson in-degree distribution and random functions is

$$h(\rho) = 2p(1-p)(1-e^{-K\rho}),$$

while the Derrida map for networks with a scale-free in-degree distribution and random functions is

$$h(\rho) = p(1-p)[1-\zeta(\gamma)\mathrm{Li}_\gamma(1-\rho)],$$

where $\mathrm{Li}_\gamma(z)$ is the polylogarithm function:

$$\mathrm{Li}_\gamma(z) = \sum_{k=1}^{\infty} \frac{z^k}{k^\gamma}.$$

We numerically tested how the in-degree distribution can change the form of the Derrida map with random functions ($p=0.5$). First, we used a typical random Boolean network with constant in-degree 2. Second, we used a network where a node has in-degree 4 with probability 1/2 and in-degree 0 with probability 1/2. This network also has average in-degree 2. Figure 2 shows the numerical and analytical Derrida maps for this test. We find that the tail of the Derrida map is considerably lower for the second test case.

Canalizing functions are a class of functions of particular interest [22]. A Boolean function f is canalizing if there is a canalizing variable x_i, $i \in 1,2,\ldots,K_f$, and s, $v \in \{0,1\}$ such that

$$\forall\ x \in \{0,1\}^{K_f}: x_i = s \Rightarrow f(x) = v.$$

Here, s is called the canalizing value and v the canalized value. For simplicity we refer to canalizing functions as $(s \to v)$-canalizing functions. We choose a parametrized distribution of canalizing functions and study the annealed dynamics of the networks generated with this distribution. All the functions of this distribution have at least one canalizing input, and this input has canalizing value 1 with probability p_1. The canalized value of the function is 1 with probability p_2. For those values in the truth table that are not determined by this canalizing input we select a random value with bias p_3; i.e., the random value is 1 with probability p_3. Note that the distribution is not limited to functions with a single canalizing input. The amount of functions with several canalizing inputs is influenced by the parameter p_3. Additional canalizing inputs can arise by chance if many noncanalized outputs happen to have an equal value.

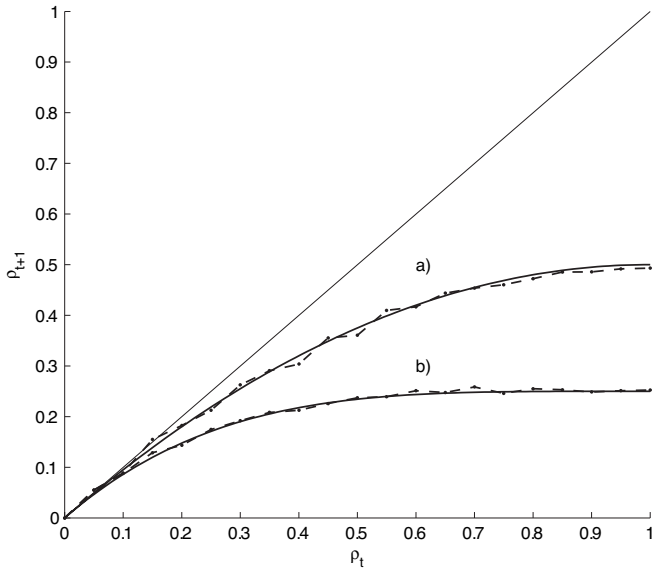

FIG. 2. Derrida maps calculated numerically (dashed lines) and analytically (solid lines). (a) The network has random functions with $p=0.5$ and constant in-degree 2. (b) The network has random functions with $p=0.5$. Half of the nodes are constant and the other half have four inputs.

For the distribution of canalizing functions we have the bias map

$$g(b) = (p_3 - p_2 + 2p_1p_2 - 2p_1p_3)b + p_2 - p_1p_2 + p_1p_3. \tag{8}$$

From this linear bias map we get a unique fixed point

$$b^* = \frac{p_2 - p_1p_2 + p_1p_3}{1 + p_2 - p_3 + 2p_1p_3 - 2p_1p_2}.$$

We get $\Delta\lambda$ by differentiating $g(b)$ as

$$\Delta\lambda = 2p_1p_2 - 2p_1p_3 - p_2 + p_3$$

and λ as

$$\lambda = (\langle p_k \rangle - 1)2p_3(1-p_3)[(1-2p_1)b^* + p_1] + p_2 + p_3 - 2p_2p_3. \tag{9}$$

Proofs of these results are in the Appendix. In particular, we have $\lambda = p_3$ if all the functions in the distribution are $0 \to 0$ canalizing ($p_1=0$, $p_2=0$) and $\lambda = 1-p_3$ if all the functions are $1 \to 1$ canalizing ($p_1=1$, $p_2=1$). In other words, networks constructed with these two function distributions are stable (or critical if all the functions are identity functions). Note

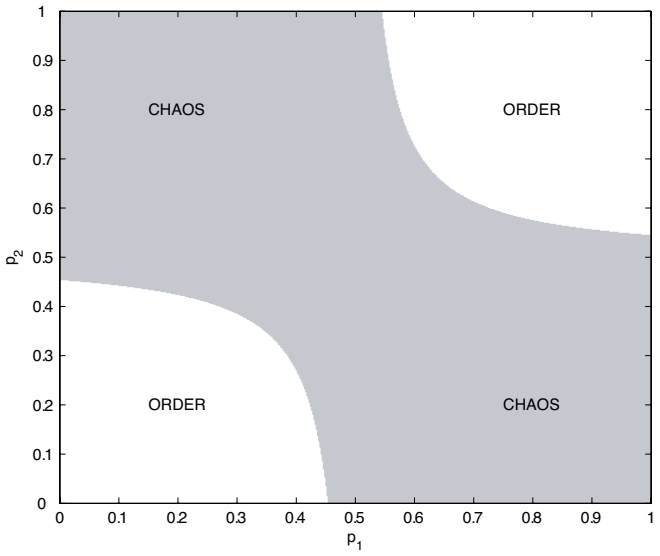

FIG. 3. (Color online) A phase transition diagram for canalizing functions when $\langle p_k \rangle = 3.1$ and $p_3 = 0.5$. p_1 and p_2 are varied.

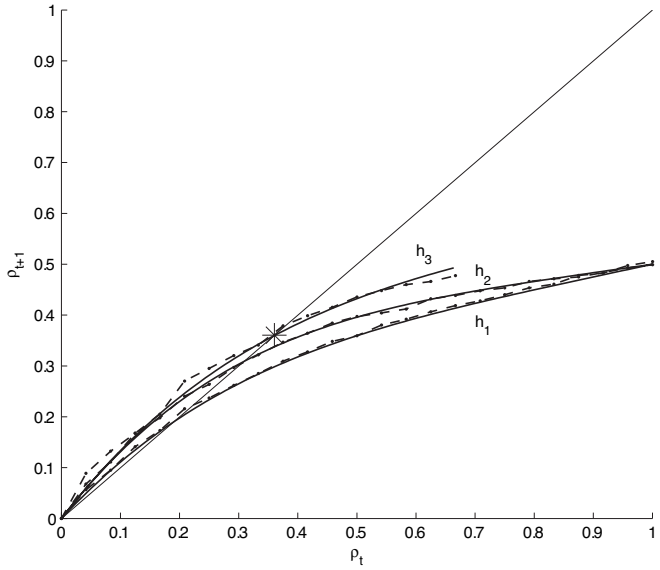

FIG. 4. Derrida maps $h_1(\rho)$, $h_2(\rho)$, and $h_3(\rho)$ calculated numerically (dashed lines) and analytically (solid lines) for canalizing functions ($p_1=0$, $p_2=1$, $p_3=0.5$, and constant in-degree $K=4$). The numerical estimate for the fixed point ρ^* is given by a star on the diagonal line.

that in these two cases the order parameter does not depend on the the average in-degree. Figure 3 shows a phase transition diagram for the distribution of canalizing functions when $\langle p_k \rangle = 3.1$, $p_3 = 0.5$, and when p_1 and p_2 are varied. The chaotic regime extends when the average in-degree gets higher and vice versa. Changing p_3 affects the position of the chaotic regime.

The Derrida maps for the distribution of canalizing functions are

$$h_1(\rho) = \sum_{k=1}^{\infty} p_k \{p_3(1-p_3)[(1-\rho)-(1-\rho)^k] + (p_3 + p_2 - 2p_2p_3)\rho\}, \tag{10}$$

$$h_2(\rho) = \sum_{k=1}^{\infty} p_k \sum_{i=1}^{k} \underset{f \in \mathfrak{F}_k}{E}[\lambda_i] \rho^i (1-\rho)^{k-i}, \tag{11}$$

where

$$\underset{f \in \mathfrak{F}_k}{E}[\lambda_i] = \binom{k-1}{i} 2p_3(1-p_3)[(1-2p_1)b^* + p_1] + \binom{k-1}{i-1} \times (p_2 + p_3 - 2p_2p_3) \tag{12}$$

and

$$h_3(\rho) = \sum_{k=1}^{\infty} p_k \left[2p_3(1-p_3)\left(p_1(1-2b^*) + b^* - \frac{1}{2}\rho\right) \times [1-(1-\rho)^{k-1}] + (p_3 + p_2 - 2p_2p_3)\rho \right]. \tag{13}$$

Proofs of these results are in the Appendix. We confirmed the applicability of the results obtained with annealed approximation by performing numerical simulations on quenched Boolean networks. We generated Boolean networks with a canalizing function distribution ($p_1=0$, $p_2=1$, $p_3=0.5$, $N=500$, and constant in-degree $K=4$). For the Derrida map $h_1(\rho)$ we choose a random state and flip a proportion of nodes ρ. Then, we run the nonperturbed and perturbed networks for one time step and calculate the average Hamming distance between the resulting states. For the Derrida map $h_2(\rho)$ we first run the network until we reach an attractor and then proceed as for $h_1(\rho)$. The Derrida map $h_3(\rho)$ is calculated similarly to $h_2(\rho)$, but we only perform perturbations that lead to a state with the same number of ones as in the original state. The theoretical and numerical results are presented in Fig. 4. In addition, we numerically calculated the fixed point ρ^* for the same function distribution by running two annealed networks in parallel. The numerical estimate is given by a star on the diagonal line in Fig. 4. We note that the Derrida maps are all different but not very far from each other in this test case. The fixed point ρ^* is correct only for the Derrida map $h_3(\rho)$.

The data set provided by Harris *et al.* [10,23] consists of 139 regulatory functions compiled and interpreted from various biological publications. These data can be used as an experimental distribution of regulatory functions. By directly using the methods presented, we obtain $b^*=0.017$, $\Delta\lambda=0.14$, and $\lambda=0.18$ for the function distribution in question. These results imply that the Boolean networks constructed using these functions are very stable and the proportion of active nodes is very low. The Derrida maps are shown in Fig. 5. It can be seen that h_1 is in significant disagreement with h_2 and h_3. It is therefore important to consider the assumptions implicitly made when interpreting network dynamics with Derrida maps. These results suggest that gene regulatory networks are rather stable. However, the regulatory functions provided by Harris *et al.* should not be considered to constitute a truly realistic function distribution of regulatory functions. In addition, any results obtained with the random to-

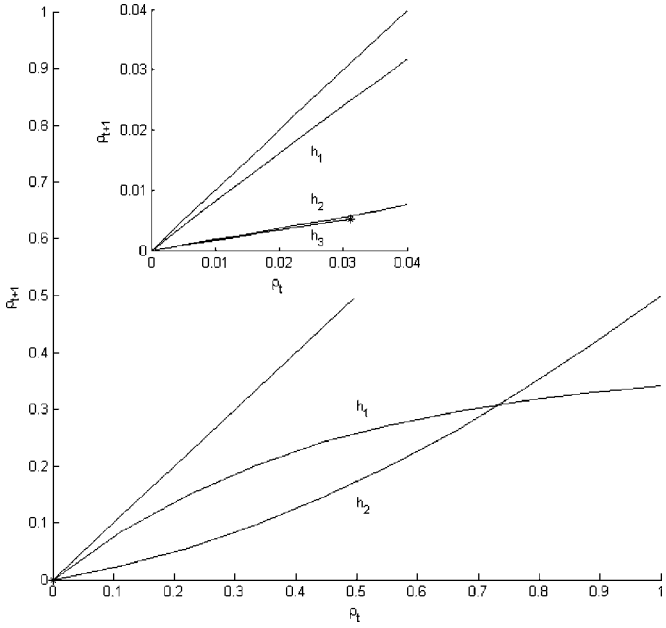

FIG. 5. Derrida maps for regulatory functions provided by Harris *et al.* in [10]. h_3 is only defined for a small range of values close to the origin due to small b^*.

pology assumption are only approximations until more accurate descriptions for the topology are found.

V. CONCLUSIONS

We have studied the annealed approximation in Boolean networks in order to present a common framework for the approaches given in the literature. Three different Derrida maps previously used can be derived from a common source, the four-state model. The most important insight gained from this study is that none of the Derrida maps can give an answer to all the questions that are of interest in the annealed model.

The limitations of the Derrida map h_1 are widely known. Its predictions fail most apparently when networks are constructed with functions that show forcing behavior—i.e., tend to drive most of the nodes to the same fixed value. The proportion of nodes that have the value 1 in this forced state is called the fixed point of the state bias. In this paper, we point out that the Derrida map h_2, which takes the forcing behavior into account, fails to correctly predict the fixed point of the perturbation size in the annealed network. In contrast, the Derrida map h_3 can be used to find the correct fixed point of the perturbation size. However, the use of the Derrida map h_3 can be limited because it might not be defined for large perturbation sizes at all.

The four-state model serves as a common basis for all the Derrida maps and can also be seen as a general way of formulating the annealed approximation. The fixed points of the iterative equations can be solved numerically for any function distribution under study or analytically for many interesting cases. For future studies with desired function distributions we suggest using the four-state model because it gives a more comprehensive dynamical analysis than any Derrida map variant.

Real genetic regulatory networks are most likely not well approximated by a network with random topology. Thus, the predictions given by the annealed model should not be expected to yield accurate predictions of the dynamical properties of cells. However, annealed dynamics can give an insight into quenched Boolean networks with random topology. Since random topology can be viewed as a null hypothesis of the network structure, the results of the annealed model can serve as a reference point for future studies. The results can be compared to results obtained with models that more accurately describe the local structures and modularity of biological networks. The development of probabilistic approximation methods to be used with topologically realistic networks remains a topic of further research.

ACKNOWLEDGMENTS

This work was supported by the Academy of Finland, Project No. 213462 (Finnish Centre of Excellence program).

APPENDIX: PROOFS FOR THE RESULTS

Proof of Eq. (1):

$$\Delta\lambda(b) = \lambda_C(b) - \lambda_I(b)$$
$$= \underset{f\in\mathfrak{F}}{E}\left[\sum_{i=1}^{K_f}\sum_{x\in\{0,1\}^{K_f}}[f(x\oplus e_i) - 2x_i f(x\oplus e_i) + 2x_i f(x) - f(x)]P(x|b)\right],$$

where we can sum two of the terms with a change of variable and the others directly:

$$\sum_{i=1}^{K_f}\sum_{x\in\{0,1\}^{K_f}} f(x\oplus e_i)P(x|b)$$
$$= \sum_{x\in\{0,1\}^{K_f}} f(x)\sum_{i=1}^{K_f} P(x\oplus e_i|b)$$
$$= \sum_{x\in\{0,1\}^{K_f}} f(x)\left[\frac{(K_f-|x|)b}{1-b} + \frac{|x|(1-b)}{b}\right]P(x|b),$$

$$\sum_{i=1}^{K_f}\sum_{x\in\{0,1\}^{K_f}} x_i f(x\oplus e_i)P(x|b)$$
$$= \sum_{x\in\{0,1\}^{K_f}} f(x)\sum_{i=1}^{K_f}[1-x_i]P(x\oplus e_i|b)$$
$$= \sum_{x\in\{0,1\}^{K_f}} f(x)\frac{(K_f-|x|)b}{1-b}P(x|b),$$

$$\sum_{i=1}^{K_f} \sum_{x\in\{0,1\}^{K_f}} x_i f(x) P(x|b) = \sum_{x\in\{0,1\}^{K_f}} f(x)|x|P(x|b),$$

and

$$\sum_{i=1}^{K_f} \sum_{x\in\{0,1\}^{K_f}} f(x) P(x|b) = \sum_{x\in\{0,1\}^{K_f}} f(x) K_f P(x|b).$$

Hence we obtain the result

$$\Delta\lambda(b) = \underset{f\in\mathfrak{F}}{E}\left[\sum_{x\in\{0,1\}^{K_f}} f(x)\frac{|x|-K_f b}{b(1-b)}P(x|b)\right] = g'(b).$$

Proof of Eq. (2): Let

$$P_{hij} = \{(x,y)|x\in\{0,1\}^{K_f}, y\in\{0,1\}^{K_f}, (1-x)^T(y) = h, x^T(1-y) = i, x^T y = j\}$$

and

$$P_{mn} = \{(x,y)|x\in\{0,1\}^{K_f}, y\in\{0,1\}^{K_f}, |x\oplus y| = m, |x| = n\};$$

then, by changing the summation variables from h, i, and j to m and n we obtain

$$\begin{aligned}
h_2(\rho) &= \underset{f\in\mathfrak{F}}{E}\left[\sum_{h=0}^{K_f}\sum_{i=0}^{K_f}\sum_{j=0}^{K_f}(1-b^*+b^*\rho-\rho)^{K_f-h-i-j}(b^*-b^*\rho)^j(\rho-b^*\rho)^h(b^*\rho)^i \sum_{(x,y)\in P_{hij}} f(x)\oplus f(y)\right] \\
&= \underset{f\in\mathfrak{F}}{E}\left[(1-\rho)^{K_f}(1-b^*)^{K_f}\sum_{h=0}^{K_f}\sum_{i=0}^{K_f}\sum_{j=0}^{K_f}\left(\frac{\rho}{1-\rho}\right)^h\left(\frac{b^*\rho}{(1-b^*)(1-\rho)}\right)^i\left(\frac{b^*}{1-b^*}\right)^j \sum_{(x,y)\in P_{hij}} f(x)\oplus f(y)\right] \\
&= \underset{f\in\mathfrak{F}}{E}\left[(1-\rho)^{K_f}(1-b^*)^{K_f}\sum_{h=0}^{K_f}\sum_{i=0}^{K_f}\sum_{j=0}^{K_f}\left(\frac{\rho}{1-\rho}\right)^{h+i}\left(\frac{b^*}{1-b^*}\right)^{i+j} \sum_{(x,y)\in P_{hij}} f(x)\oplus f(y)\right] \\
&= \underset{f\in\mathfrak{F}}{E}\left[(1-\rho)^{K_f}(1-b^*)^{K_f}\sum_{m=0}^{K_f}\sum_{n=0}^{K_f}\left(\frac{\rho}{1-\rho}\right)^m\left(\frac{b^*}{1-b^*}\right)^n \sum_{(x,y)\in P_{mn}} f(x)\oplus f(y)\right] \\
&= \underset{f\in\mathfrak{F}}{E}\left[\sum_{y\in\{0,1\}^{K_f}}\sum_{x\in\{0,1\}^{K_f}}[f(x)\oplus f(y)]b^{*|x|}(1-b^*)^{K_f-|x|}\rho^{|x\oplus y|}(1-\rho)^{K_f-|x\oplus y|}\right] \\
&= \underset{f\in\mathfrak{F}}{E}\left[\sum_{k=1}^{K_f}\sum_{y\in P_k}\sum_{x\in\{0,1\}^{K_f}}[f(x)\oplus f(x\oplus y)]b^{*|x|}(1-b^*)^{K_f-|x|}\rho^k(1-\rho)^{K_f-k}\right] \\
&= \underset{f\in\mathfrak{F}}{E}\left[\sum_{k=1}^{K_f}\lambda_k\rho^k(1-\rho)^{K_f-k}\right].
\end{aligned}$$

Proof of Eq. (3): From $b^*=0$ we get

$$\sum_{x\in\{0,1\}^{K_f}} f(x)P(x|0) = 0 \Rightarrow f(0) = 0.$$

Therefore,

$$\lambda_k = \sum_{y\in P_k}\sum_{x\in\{0,1\}^{K_f}}[f(x)\oplus f(x\oplus y)]P(x|0) = \sum_{y\in P_k} f(y)$$

and

$$\begin{aligned}
h_2(\rho) &= \underset{f\in\mathfrak{F}}{E}\left[\sum_{k=1}^{K_f}\sum_{y\in P_k} f(y)\rho^k(1-\rho)^{K_f-k}\right] \\
&= \underset{f\in\mathfrak{F}}{E}\left[\sum_{x\in\{0,1\}^{K_f}} f(x)\rho^{|x|}(1-\rho)^{K_f-|x|}\right] = g(\rho).
\end{aligned}$$

Proof of Eq. (4): We note that after differentiating $h_1'(0)$ all the terms with $|x\oplus y|$ larger than 1 will go to zero. Thus,

$$\begin{aligned}
h_1'(0) &= \underset{f\in\mathfrak{F}}{E}\left[\sum_{\substack{x\in\{0,1\}^{K_f}\\ |x\oplus y|=1}}\sum_{y\in\{0,1\}^{K_f}}[f(x)\oplus f(y)]\left(\frac{1}{2}\right)^{K_f}\right] \\
&= \underset{f\in\mathfrak{F}}{E}\left[\sum_{i=1}^{K_f}\sum_{x\in\{0,1\}^{K_f}}[f(x)\oplus f(x\oplus e_i)]\left(\frac{1}{2}\right)^{K_f}\right] = \lambda\left(\frac{1}{2}\right).
\end{aligned}$$

Proof of Eq. (5): By differentiating Eq. (2) we obtain

$$h_2'(\rho) = \underset{f\in\mathfrak{F}}{E}\left[\sum_{k=1}^{K_f}\lambda_k[k\rho^{k-1}(1-\rho)^{K_f-k} - (K_f-k)\rho^k(1-\rho)^{K_f-k-1}]\right].$$

When we set $\rho=0$ in this formula we note that all the terms except that corresponding to $k=1$ will go to zero. Hence

$$h_2'(0) = \underset{f\in\mathfrak{F}}{E}[\lambda_1] = \lambda.$$

By differentiating and splitting the resulting summations into two parts we get

$$\begin{aligned}
h_3'(0) &= \frac{1}{2}\underset{f\in\mathfrak{F}}{E}\left[\sum_{i=1}^{K_f}\sum_{x\in\{0,1\}^{K_f}}[f(x)\oplus f(x\oplus e_i)]b^{x^T(x\oplus e_i)}(1-b)^{(1-x)^T(1-x\oplus e_i)}\right] \\
&= \frac{1}{2}\underset{f\in\mathfrak{F}}{E}\left\{\sum_{i=1}^{K_f}\left[\sum_{\substack{x\in\{0,1\}^{K_f}\\ x_i=0}}[f(x)\oplus f(x\oplus e_i)]b^{|x|}(1-b)^{K_f-|x|-1}+\sum_{\substack{x\in\{0,1\}^{K_f}\\ x_i=1}}[f(x)\oplus f(x\oplus e_i)]b^{|x|-1}(1-b)^{K_f-|x|}\right]\right\} \\
&= \frac{1}{2}\underset{f\in\mathfrak{F}}{E}\left\{\sum_{i=1}^{K_f}\left[\sum_{\substack{x\in\{0,1\}^{K_f}\\ x_i=0}}[f(x)\oplus f(x\oplus e_i)]b^{|x|}(1-b)^{K_f-|x|-1}+\sum_{\substack{x\in\{0,1\}^{K_f}\\ x_i=0}}[f(x\oplus e_i)\oplus f(x)]b^{|x|}(1-b)^{K_f-|x|-1}\right]\right\} \\
&= \underset{f\in\mathfrak{F}}{E}\left[\frac{1}{1-b}\sum_{i=1}^{K_f}\sum_{\substack{x\in\{0,1\}^{K_f}\\ x_i=0}}[f(x)\oplus f(x\oplus e_i)]b^{|x|}(1-b)^{K_f-|x|}\right] \\
&= \underset{f\in\mathfrak{F}}{E}\left\{\sum_{i=1}^{K_f}\left[\sum_{\substack{x\in\{0,1\}^{K_f}\\ x_i=0}}[f(x)\oplus f(x\oplus e_i)]b^{|x|}(1-b)^{K_f-|x|}+\sum_{\substack{x\in\{0,1\}^{K_f}\\ x_i=0}}[f(x\oplus e_i)\oplus f(x)]b^{|x|+1}(1-b)^{K_f-|x|-1}\right]\right\} \\
&= \underset{f\in\mathfrak{F}}{E}\left\{\sum_{i=1}^{K_f}\left[\sum_{\substack{x\in\{0,1\}^{K_f}\\ x_i=0}}[f(x)\oplus f(x\oplus e_i)]b^{|x|}(1-b)^{K_f-|x|}+\sum_{\substack{x\in\{0,1\}^{K_f}\\ x_i=1}}[f(x)\oplus f(x\oplus e_i)]b^{|x|}(1-b)^{K_f-|x|}\right]\right\} \\
&= \underset{f\in\mathfrak{F}}{E}\left[\sum_{i=1}^{K_f}\sum_{x\in\{0,1\}^{K_f}}[f(x)\oplus f(x\oplus e_i)]b^{|x|}(1-b)^{K_f-|x|}\right] = \lambda.
\end{aligned}$$

Here it is helpful to note that perturbing a single, ith bit, of state x will either increase or decrease $|x|$ by one depending on the value x_i.

Proof of Eq. (6):

$$g(b) = \underset{f\in\mathfrak{F}}{E}\left[\sum_{x\in\{0,1\}^{K_f}} f(x)P(x|b)\right] = \sum_{k=1}^{\infty} p_k \sum_{x\in\{0,1\}^k} \underset{f\in\mathfrak{F}_k}{E}[f(x)]P(x|b) = p\sum_{k=1}^{\infty} p_k \sum_{x\in\{0,1\}^k} P(x|b) = p.$$

Both summations will give one as a result since they are summations of probabilities over all the possible outcomes.

Proof of Eq. (7):

$$\begin{aligned}
\lambda(b) &= \underset{f\in\mathfrak{F}}{E}\left[\sum_{i=1}^{K_f}\sum_{x\in\{0,1\}^{K_f}}[f(x)\oplus f(x\oplus e_i)]P(x|b)\right] = \sum_{k=1}^{\infty} p_k \sum_{i=1}^{k}\sum_{x\in\{0,1\}^k}\underset{f\in\mathfrak{F}_k}{E}[f(x)\oplus f(x\oplus e_i)]P(x|b) = 2p(1 \\
&\quad - p)\sum_{k=1}^{\infty} p_k \sum_{i=1}^{k}\sum_{x\in\{0,1\}^k} P(x|b) = 2p(1-p)\langle p_k\rangle,
\end{aligned}$$

where $E_{f\in\mathfrak{F}_k}[f(x)\oplus f(x\oplus e_i)]=2p(1-p)$ for all x and i since the outputs of f are selected independently with bias p.

Proof of Eq. (7): According to the binomial theorem we have

$$\sum_{i=0}^{K}\binom{K}{i}a^i = (1+a)^K$$

and

$$\sum_{i=1}^{K} \binom{K}{i} a^i = (1+a)^K - 1.$$

Using these formulas we can obtain the three Derrida maps for random functions as follows.

Derrida map $h_1(\rho)$:

$$\begin{aligned}
h_1(\rho) &= \sum_{k=1}^{\infty} p_k \sum_{x\in\{0,1\}^k} \sum_{i=1}^{k} \sum_{y\in P_i} \underset{f\in\mathfrak{F}_k}{E}[f(x)\oplus f(x\oplus y)] \left(\frac{1}{2}\rho\right)^i \left(\frac{1}{2}-\frac{1}{2}\rho\right)^{k-i} \\
&= 2p(1-p)\sum_{k=1}^{\infty} p_k \left(\frac{1}{2}-\frac{1}{2}\rho\right)^k \sum_{x\in\{0,1\}^k} \sum_{i=1}^{k} \binom{k}{i} \left(\frac{\frac{1}{2}\rho}{\frac{1}{2}-\frac{1}{2}\rho}\right)^i \\
&= 2p(1-p)\sum_{k=1}^{\infty} p_k \left(\frac{1}{2}-\frac{1}{2}\rho\right)^k 2^k \left[\left(1+\frac{\rho}{1-\rho}\right)^k - 1\right] \\
&= 2p(1-p)\sum_{k=1}^{\infty} p_k [1-(1-\rho)^k].
\end{aligned}$$

Derrida map $h_2(\rho)$:

$$\begin{aligned}
h_2(\rho) &= \sum_{k=1}^{\infty} p_k \sum_{i=1}^{k} \underset{f\in\mathfrak{F}_k}{E}[\lambda_i] \rho^i (1-\rho)^{k-i} \\
&= 2p(1-p)\sum_{k=1}^{\infty} p_k \sum_{i=1}^{k} \binom{k}{i} \rho^i (1-\rho)^{k-i} \\
&= 2p(1-p)\sum_{k=1}^{\infty} p_k (1-\rho)^k \sum_{i=1}^{k} \binom{k}{i} \left(\frac{\rho}{1-\rho}\right)^i \\
&= 2p(1-p)\sum_{k=1}^{\infty} p_k (1-\rho)^k \left[\left(1-\frac{\rho}{1-\rho}\right)^k - 1\right] \\
&= 2p(1-p)\sum_{k=1}^{\infty} p_k [1-(1-\rho)^k].
\end{aligned}$$

Derrida map $h_3(\rho)$:

$$\begin{aligned}
h_3(\rho) &= \sum_{k=1}^{\infty} p_k \sum_{\substack{x\in\{0,1\}^k \\ x\neq y}} \sum_{y\in\{0,1\}^k} \underset{f\in\mathfrak{F}_k}{E}[f(x)\oplus f(y)] \left(1-p-\frac{1}{2}\rho\right)^{(1-x)^T(1-y)} \left(p-\frac{1}{2}\rho\right)^{x^T y} \left(\frac{1}{2}\rho\right)^{|x\oplus y|} \\
&= 2p(1-p)\sum_{k=1}^{\infty} p_k \sum_{i=1}^{k} \sum_{j=0}^{k-i} \binom{k}{i} \binom{k-i}{j} \left(1-p-\frac{1}{2}\rho\right)^{k-i-j} \left(p-\frac{1}{2}\rho\right)^j \left(\frac{1}{2}\rho\right)^i 2^i \\
&= 2p(1-p)\sum_{k=1}^{\infty} p_k \left(1-p-\frac{1}{2}\rho\right)^k \sum_{i=1}^{k} \binom{k}{i} \left(\frac{\rho}{1-p-\frac{1}{2}\rho}\right)^i \sum_{j=0}^{k-i} \binom{k-i}{j} \left(\frac{p-\frac{1}{2}\rho}{1-p-\frac{1}{2}\rho}\right)^j \\
&= 2p(1-p)\sum_{k=1}^{\infty} p_k \left(1-p-\frac{1}{2}\rho\right)^k \sum_{i=1}^{k} \binom{k}{i} \left(\frac{\rho}{1-p-\frac{1}{2}\rho}\right)^i \left(1+\frac{p-\frac{1}{2}\rho}{1-p-\frac{1}{2}\rho}\right)^{k-i}
\end{aligned}$$

$$= 2p(1-p)\sum_{k=1}^{\infty} p_k(1-\rho)^k \sum_{i=1}^{k} \binom{k}{i} \left(\frac{\rho}{1-\rho}\right)^i$$

$$= 2p(1-p)\sum_{k=1}^{\infty} p_k(1-\rho)^k \left[\left(1+\frac{\rho}{1-\rho}\right)^k - 1\right]$$

$$= 2p(1-p)\sum_{k=1}^{\infty} p_k[1-(1-\rho)^k].$$

Proof of Equation (10): We first note that

$$\sum_{\substack{x\in\{0,1\}^K \\ x_1=0}} P(x|b) = (1-b) \sum_{x\in\{0,1\}^{K-1}} b^{|x|}(1-b)^{K-1-|x|} = 1-b,$$

where the latter sum can be seen to be equal to 1 since it is the sum of probabilities over all vectors in a distribution of $(K-1)$-dimensional vectors and, similarly,

$$\sum_{\substack{x\in\{0,1\}^K \\ x_1=1}} P(x|b) = b.$$

Without loss of generality we can assume that the first variable is the canalizing variable. Then,

$$g(b) = \underset{f\in\mathfrak{F}}{E}\left[\sum_{x\in\{0,1\}^{K_f}} f(x)P(x|b)\right] = \sum_{k=1}^{\infty} p_k \sum_{\substack{x\in\{0,1\}^k \\ x_1=0}} \underset{f\in\mathfrak{F}_k}{E}[f(x)]P(x|b) + \sum_{k=1}^{\infty} p_k \sum_{\substack{x\in\{0,1\}^k \\ x_1=1}} \underset{f\in\mathfrak{F}_k}{E}[f(x)]P(x|b)$$

$$= [(1-p_1)p_2 + p_1p_3]\sum_{k=1}^{\infty} p_k \sum_{\substack{x\in\{0,1\}^k \\ x_1=0}} P(x|b) + [p_1p_2 + (1-p_1)p_3]\sum_{k=1}^{\infty} p_k \sum_{\substack{x\in\{0,1\}^k \\ x_1=1}} P(x|b)$$

$$= [(1-p_1)p_2 + p_1p_3](1-b) + [p_1p_2 + (1-p_1)p_3]b = (p_3 - p_2 + 2p_1p_2 - 2p_1p_3)b + p_2 - p_1p_2 + p_1p_3.$$

Here, e.g., when $x_1=0$, we have

$$\underset{f\in\mathfrak{F}_k}{E}[f(x)] = (1-p_1)p_2 + p_1p_3,$$

where the first product is the probability that f has canalizing zero and is therefore canalized and the canalized value is 1, and the second product is the probability that f is not canalized, i.e., the canalizing value is 1, and the function f obtains value 1 with probability p_3. The another expected value can be obtained in a similar way.

Proof of Eqs. (10) and (13): We solve first the general case of $\lambda_k(b)$ for canalizing functions with constant in-degree K. We first divide the sum of the definition into four parts,

$$\underset{f\in\mathfrak{F}_K}{E}[\lambda_k(b)] = \underset{f\in\mathfrak{F}_K}{E}\left[\sum_{x\in\{0,1\}^K}\sum_{y\in P_k} f(x)\oplus f(x\oplus y)P(x|b)\right]$$

$$= \sum_{\substack{x\in\{0,1\}^k \\ x_1=0}} \left[\sum_{\substack{y\in P_k \\ y_1=1}} \underset{f\in\mathfrak{F}_K}{E}[f(x)\oplus f(x\oplus y)] + \sum_{\substack{y\in P_k \\ y_1=0}} \underset{f\in\mathfrak{F}_K}{E}[f(x)\oplus f(x\oplus y)]\right] P(x|b)$$

$$+ \sum_{\substack{x\in\{0,1\}^K \\ x_1=1}} \left[\sum_{\substack{y\in P_k \\ y_1=1}} \underset{f\in\mathfrak{F}_K}{E}[f(x)\oplus f(x\oplus y)] + \sum_{\substack{y\in P_k \\ y_1=0}} \underset{f\in\mathfrak{F}_K}{E}[f(x)\oplus f(x\oplus y)]\right] P(x|b).$$

The expectations can be computed by taking all the cases where $f(x)$ and $f(x\oplus y)$ differ and adding up their probabilities that can be computed from the probabilities that functions have specific canalizing and canalized values and the bias p_3. In the first case, for example, there are then $\binom{K-1}{k-1}$ ways to choose the $k-1$ bits of y that are not fixed by condition $y_1=1$. In this way, the inner sum can be computed. We obtain

$$\begin{aligned}
\underset{f\in\mathfrak{F}_K}{E}[\lambda_k(b)] &= \sum_{\substack{x\in\{0,1\}^K \\ x_1=0}} \left[\binom{K-1}{k-1} [(1-p_1)(1-p_2)p_3 + (1-p_1)p_2(1-p_3) + p_1(1-p_2)p_3 + p_1(1-p_2)p_3 + p_1p_2(1-p_3)] + \binom{K-1}{k} \right. \\
&\left. \times [p_1(1-p_2)2p_3(1-p_3) + p_1p_2 2p_3(1-p_3)] \right] P(x|b) + \sum_{\substack{x\in\{0,1\}^K \\ x_1=1}} \left[\binom{K-1}{k-1} [(1-p_1)(1-p_2)p_3 + (1-p_1)p_2(1-p_3) \right. \\
&+ p_1(1-p_2)p_3 + p_1(1-p_2)p_3 + p_1p_2(1-p_3)] + \binom{K-1}{k} [(1-p_1)(1-p_2)2p_3(1-p_3) + (1-p_1)p_2 2p_3(1 \\
&\left. - p_3)] \right] P(x|b) \\
&= \binom{K-1}{k} 2p_3(1-p_3)[(1-2p_1)b + p_1] + \binom{K-1}{k-1}(p_2 + p_3 - 2p_2p_3).
\end{aligned}$$

This proves Eq. (13) and the result for $\lambda(b)$ in Eq. (10) follows by considering the special case $k=1$ and taking the expectation with respect to a distribution of in-degrees.

Proof of Eq. (12):

$$\begin{aligned}
h_1(\rho) &= \underset{f\in\mathfrak{F}}{E}\left[\sum_{x\in\{0,1\}^{K_f}} \sum_{y\in\{0,1\}^{K_f}} [f(x)\oplus f(y)] \left(\frac{1}{2} - \frac{1}{2}\rho\right)^{K_f - |x\oplus y|} \left(\frac{1}{2}\rho\right)^{|x\oplus y|} \right] \\
&= \sum_{k=1}^{\infty} p_k \sum_{\substack{x\in\{0,1\}^k: \\ x_1=0}} \sum_{\substack{y\in\{0,1\}^k: \\ y_1=0}} \underset{f\in\mathfrak{F}_k}{E}[f(x)\oplus f(y)] \left(\frac{1}{2} - \frac{1}{2}\rho\right)^{k-|x\oplus y|} \left(\frac{1}{2}\rho\right)^{|x\oplus y|} + 2\sum_{k=1}^{\infty} p_k \sum_{\substack{x\in\{0,1\}^k \\ x_1\neq y_1}} \sum_{y\in\{0,1\}^k} \underset{f\in\mathfrak{F}_k}{E}[f(x)\oplus f(y)] \\
&\times \left(\frac{1}{2} - \frac{1}{2}\rho\right)^{k-|x\oplus y|} \left(\frac{1}{2}\rho\right)^{|x\oplus y|} + \sum_{k=1}^{\infty} p_k \sum_{\substack{x\in\{0,1\}^k: \\ x_1=1}} \sum_{\substack{y\in\{0,1\}^k: \\ y_1=1}} \underset{f\in\mathfrak{F}_k}{E}[f(x)\oplus f(y)] \left(\frac{1}{2} - \frac{1}{2}\rho\right)^{k-|x\oplus y|} \left(\frac{1}{2}\rho\right)^{|x\oplus y|} \\
&= \sum_{k=1}^{\infty} p_k \{p_3(1-p_3)[(1-\rho) - (1-\rho)^k] + (p_3 + p_2 - 2p_2p_3)\rho\},
\end{aligned}$$

since when $x_1 \neq y_1$,

$$\underset{f\in\mathfrak{F}_k}{E}[f(x)\oplus f(y)] = p_3 + p_2 - 2p_2p_3,$$

and when $x_1 = y_1 = 0$, $x \neq y$,

$$\underset{f\in\mathfrak{F}_k}{E}[f(x)\oplus f(y)] = 2p_3(1-p_3)p_1,$$

and when $x_1 = y_1 = 1$, $x \neq y$,

$$\underset{f\in\mathfrak{F}_k}{E}[f(x)\oplus f(y)] = 2p_3(1-p_3)(1-p_1),$$

and

$$\begin{aligned}
\sum_{\substack{x\in\{0,1\}^k \\ x_1=y_1, x\neq y}} \sum_{y\in\{0,1\}^k} \left(\frac{1}{2} - \frac{1}{2}\rho\right)^{k-|x\oplus y|} \left(\frac{1}{2}\rho\right)^{|x\oplus y|} &= \left(\frac{1}{2} - \frac{1}{2}\rho\right)^k \sum_{x\in\{0,1\}^{k-1}} \sum_{i=1}^{k-1} \binom{k-1}{i} \left(\frac{\frac{1}{2}\rho}{\frac{1}{2} - \frac{1}{2}\rho}\right)^i = \left(\frac{1}{2} - \frac{1}{2}\rho\right)^k 2^{k-1} \left[\left(1 + \frac{\rho}{1-\rho}\right)^{k-1} - 1 \right] \\
&= \frac{1}{2}[(1-\rho) - (1-\rho)^k],
\end{aligned}$$

and

$$\sum_{\substack{x\in\{0,1\}^k \\ x_1\neq y_1}}\sum_{y\in\{0,1\}^k}\left(\frac{1}{2}-\frac{1}{2}\rho\right)^{k-|x\oplus y|}\left(\frac{1}{2}\rho\right)^{|x\oplus y|}=\frac{1}{2}\rho\left(\frac{1}{2}-\frac{1}{2}\rho\right)^{k-1}\sum_{x\in\{0,1\}^{k-1}}\sum_{i=0}^{k-1}\binom{k-1}{i}\left(\frac{\frac{1}{2}\rho}{\frac{1}{2}-\frac{1}{2}\rho}\right)^{i}=\frac{1}{2^k}\rho(1-\rho)^{k-1}2^{k-1}\left(1+\frac{\rho}{1-\rho}\right)^{k-1}$$

$$=\frac{1}{2}\rho.$$

Proof of Eq. (12): By noting that we can apply linearity of expectation we obtain

$$h_2(\rho)=\underset{f\in\mathfrak{F}}{E}\left[\sum_{i=1}^{K_f}\lambda_i\rho^i(1-\rho)^{K_f-i}\right]=\sum_{k=1}^{\infty}p_k\sum_{i=1}^{k}\underset{f\in\mathfrak{F}_k}{E}[\lambda_i]\rho^i(1-\rho)^{k-i}.$$

Proof of Eq. (13): Utilizing the expected values mentioned in the proof of Eq. (11) we have

$$h_3(\rho)=\sum_{k=1}^{\infty}p_k\sum_{x\in\{0,1\}^k}\sum_{y\in\{0,1\}^k}\underset{f\in\mathfrak{F}_k}{E}[f(x)\oplus f(y)]\left(1-b^*-\frac{1}{2}\rho\right)^{(1-x)^T(1-y)}\left(b^*-\frac{1}{2}\rho\right)^{x^Ty}\left(\frac{1}{2}\rho\right)^{|x\oplus y|}$$

$$=\sum_{k=1}^{\infty}p_k\sum_{\substack{x\in\{0,1\}^k: \\ x_1=0}}\sum_{\substack{y\in\{0,1\}^k: \\ y_1=0}}\underset{f\in\mathfrak{F}_k}{E}[f(x)\oplus f(y)]\left(1-b^*-\frac{1}{2}\rho\right)^{(1-x)^T(1-y)}\left(b^*-\frac{1}{2}\rho\right)^{x^Ty}\left(\frac{1}{2}\rho\right)^{|x\oplus y|}+2\sum_{k=1}^{\infty}p_k\sum_{\substack{x\in\{0,1\}^k \\ x_1\neq y_1}}\sum_{y\in\{0,1\}^k}\underset{f\in\mathfrak{F}_k}{E}[f(x)$$

$$\oplus f(y)]\left(1-b^*-\frac{1}{2}\rho\right)^{(1-x)^T(1-y)}\left(b^*-\frac{1}{2}\rho\right)^{x^Ty}\left(\frac{1}{2}\rho\right)^{|x\oplus y|}+\sum_{k=1}^{\infty}p_k\sum_{\substack{x\in\{0,1\}^k: \\ x_1=1}}\sum_{\substack{y\in\{0,1\}^k: \\ y_1=1}}$$

$$\times\underset{f\in\mathfrak{F}_k}{E}[f(x)\oplus f(y)]\left(1-b^*-\frac{1}{2}\rho\right)^{(1-x)^T(1-y)}\left(b^*-\frac{1}{2}\rho\right)^{x^Ty}\left(\frac{1}{2}\rho\right)^{|x\oplus y|}$$

$$=\sum_{k=1}^{\infty}p_k2p_3(1-p_3)p_1\left(1-b^*-\frac{1}{2}\rho\right)\sum_{i=1}^{k-1}\sum_{j=0}^{k-1-i}\binom{k-1}{i}\binom{k-1-i}{j}2^i\left(1-b^*-\frac{1}{2}\rho\right)^{k-1-i-j}\left(b^*-\frac{1}{2}\rho\right)^j\left(\frac{1}{2}\rho\right)^i$$

$$+\sum_{k=1}^{\infty}p_k2(p_3+p_2-2p_2p_3)\left(\frac{1}{2}\rho\right)\sum_{i=0}^{k-1}\sum_{j=0}^{k-1-i}\binom{k-1}{i}\binom{k-1-i}{j}2^i\left(1-b^*-\frac{1}{2}\rho\right)^{k-1-i-j}\left(b^*-\frac{1}{2}\rho\right)^j\left(\frac{1}{2}\rho\right)^i+\sum_{k=1}^{\infty}p_k2p_3(1-p_3)$$

$$\times(1-p_1)\left(b^*-\frac{1}{2}\rho\right)\sum_{i=1}^{k-1}\sum_{j=0}^{k-1-i}\binom{k-1}{i}\binom{k-1-i}{j}2^i\left(1-b^*-\frac{1}{2}\rho\right)^{k-1-i-j}\left(b^*-\frac{1}{2}\rho\right)^j\left(\frac{1}{2}\rho\right)^i.$$

Using the binomial theorem we obtain

$$h_3(\rho)=\sum_{k=1}^{\infty}p_k\left\{2p_3(1-p_3)\left[p_1(1-2b^*)+b^*-\frac{1}{2}\rho\right][1-(1-\rho)^{k-1}]+(p_3+p_2-2p_2p_3)\rho\right\}.$$

[1] S. Kauffman, J. Theor. Biol. **22**, 437 (1969).

[2] S. Kauffman, *The Origins of Order* (Oxford University Press, New York, 1993).

[3] M. Aldana, S. Coppersmith, and L. P. Kadanoff, in *Perspectives and Problems in Nonlinear Science*, edited by E. Kaplan, J. E. Marsden, and K. R. Sreenivasan (Springer, Berlin, 2003), pp. 23–89.

[4] I. Shmulevich, S. Kauffman, and M. Aldana, Proc. Natl. Acad. Sci. U.S.A. **102**, 13439 (2005).

[5] P. Rm, J. Kesseli, and O. Yli-Harja, J. Theor. Biol. (to be published).

[6] B. Derrida and Y. Pomeau, Europhys. Lett. **1**, 45 (1986).

[7] B. Derrida and D. Stauffer, Europhys. Lett. **2**, 739 (1986).

[8] I. Shmulevich, H. Lähdesmäki, E. R. Dougherty, J. Astola, and W. Zhang, Proc. Natl. Acad. Sci. U.S.A. **100**, 10734 (2003).

[9] I. Shmulevich and S. A. Kauffman, Phys. Rev. Lett. **93**, 048701 (2004).

[10] S. Harris, B. Sawhill, A. Wuenche, and S. Kauffman, Complexity **7**, 23 (2001).

[11] A. Moreira, L. Amaral, and Lusis A. Nuues, Phys. Rev. Lett. **94**, 218702 (2005).
[12] J. Kesseli, P. Rämö, and O. Yli-Harja, Phys. Rev. E **72**, 026137 (2005).
[13] B. Samuelsson and C. Troein, Phys. Rev. E **72**, 046112 (2005).
[14] B. Drossel, T. Mihaljev, and F. Greil, Phys. Rev. Lett. **94**, 088701 (2005).
[15] T. Lee *et al.*, Science **298**, 799 (2002).
[16] M. Aldana, Physica D **185**, 45 (2003).
[17] P. Rämö, J. Kesseli, and O. Yli-Harja, Chaos **15**, 034101 (2005).
[18] M. T. Matache and J. Heidel, Phys. Rev. E **69**, 056214 (2004).
[19] M. Andrecut and M. K. Ali, Int. J. Mod. Phys. B **15**, 17 (2001).
[20] M. Andrecut, J. Stat. Mech. Theory Exp. **2005**, P02003 (2005).
[21] A. Bernasconi, Ph. D. thesis, University of Pisa, 1998.
[22] W. Just, I. Shmulevich, and J. Konvalina, Physica D **197**, 211 (2004).
[23] S. Kauffman, C. Peterson, B. Samuelsson, and C. Troein, Proc. Natl. Acad. Sci. U.S.A. **100**, 14796 (2003).